MedChemComm

Accepted Manuscript

ROYAL SOCIETY OF CHEMISTRY

www.rsc.org/medchemcomm

New selective A_{2A} agonists and A_3 antagonists for human adenosine receptors. Synthesis, biological activity and molecular docking studies

Anna Rodríguez,[a] Angel Guerrero,*[a] Hugo Gutierrez-de-Terán,[b] David Rodríguez,[c] José Brea,[d] María I. Loza,[d] Gloria Rosell,[e] M. Pilar Bosch,*[a]

[a]*Dept. of Biological Chemistry and Molecular Modelling, IQAC (C.S.I.C.), 08034-Barcelona, Spain.*

[b]*Dept. of Cell and Molecular Biology, Uppsala University, Biomedical Center, Box 596, SE-751 24 Uppsala, Sweden.*

[c]*Dept. of Biochemistry and Biophysics and Center for Biomembrane Research, Stockholm University, SE-106 91 Stockholm, Sweden.*

[d]*Biofarma research group. Center of Research in Molecular Medicine and Chronic Diseases (CIMUS), 15782-Santiago de Compostela, Spain.*

[e]*Dept. of Pharmacology and Medicinal Chemistry (Unity Associated to CSIC), Fac. Pharmacy, University of Barcelona, Av. Diagonal, s/n, 08028-Barcelona, Spain.*

*Corresponding authors. Tel.: +34 934006120 (A.G.), tel.: +34 934006171 (P.B.); fax: +34 932045904. E-mail: angel.guerrero@iqac.csic.es (A. Guerrero); pilar.bosch@iqac.csic.es (M. Pilar Bosch)

Abstract

We report the synthesis and pharmacological characterization of a new series of adenosine derivatives on the four adenosine receptors (AR). In radioligand binding assays, some of the compounds (**1**, **4**, **6** and (*R*)-**6**) display a potent affinity for the A_{2A}AR (K_i values <10 nM) with high A_1/A_{2A} and A_{2B}/A_{2A} selectivity, moderate for the A_3AR and low for the A_1AR. The affinity of the epimeric mixture **6** was similar to that of the corresponding (*R*)-**6** stereoisomer and 10-fold higher than that of the (*S*)-**6** stereoisomer. The phenylethylamino group appears to play a key role on the activity but introduction of groups of different size and electronegativity does not induce a substantial change in affinity for the A_{2A}AR. In functional assays, most of the compounds produced similar amounts of cAMP compared to NECA, thus behaving as full A_{2A}AR agonists. Also, compounds **1**, **2**, **3**, **5**, (*S*)-**6** and **9** resulted good antagonists for A_3AR with K_B in 6-14 nM range. Docking studies on the A_{2A}AR showed a conserved binding mode consistent with previous A_{2A}AR agonist-bound crystal structures, allowing for a rational interpretation of the SAR of this compound series.

Keywords: Adenosine receptors, Agonists, Antagonists, Binding affinity, Biological activity, Ligand selectivity, Molecular docking.

Adenosine is a ubiquitous purine nucleoside that mediates a range of physiological processes, such as those related to the cardiovascular system, kidney, CNS, cancer, inflammation, etc. through activation of the adenosine receptors (ARs).[1-5] Four ARs exist, namely A_1, A_{2A}, A_{2B} and A_3, all belonging to the class-A (rhodopsin-like) family of G-protein coupled receptors (GPCRs).[6] All four ARs regulate the activity of adenylyl cyclase, stimulating (A_{2A} and A_{2B}, coupled to G_s) or inhibiting (A_1 and A_3, coupled to $G_{i/o}$) production of intracellular cAMP.[6]

Most AR agonists reported to date are based on the chemical scaffold of adenosine. Modifications tolerated for preserving agonist activity include those involving the 5' and 2' positions of the ribose moiety, as well as substitutions at the C2 and N6 positions of the adenine group of the natural agonist.[7, 8] As a result, a plethora of A_{2A}AR agonists have been published in the last years.[9-11] The recent structures of active-like A_{2A}AR[12, 13] allow for a deep understanding of the process of molecular recognition of AR agonists,[14] providing excellent opportunities for structure-based, computer-aided ligand design.[15] Despite these recent developments, A_{2A}AR agonists with a strong selectivity profile are still to be developed.[8]

In a previous work we prepared and tested a range of A_{2A}AR agonists with potent affinities and improved A_1/A_{2A} and A_3/A_{2A} selectivities.[16] All compounds contained a hydroxymethyl group at 1-position of the *p*-substituted phenylethylamino moiety except compound (*R*)-**6** (compound **1** in Chart 1) that contained a methyl group. We found[16] that substitution at the *para* position of the phenyl ring notably increased the binding affinity for the A_{2A}AR and at the same time reduced the affinity for A_1AR and A_3AR. Particularly notable was the activity of compound (*R*)-**6** which improved the A_1/A_{2A} and A_3/A_{2A} selectivity to 356- and 100-fold against A_1 and A_3, respectively. Encouraged by this result, we present herein the synthesis, biological activity and molecular docking studies of the methyl analogues **1**-**7** as epimeric mixtures at the C1 side chain of the 2-position of the purine, as well as those of stereoisomer (*S*)-**6**, not previously described, as new A_{2A} agonists and A_3 antagonists for human adenosine receptors. In

addition, compounds **8**-**10** with different substituents at positions 2 and 5' of the adenosine were also prepared and tested (Chart 1).

For the synthesis of compounds **1**-**7** we followed a similar approach as previously described[16] (Scheme 1). Compound **11** was obtained from (D)-ribose in 42% overall yield in 5 steps.[16] Introduction of the ethyl group at N-2 of the tetrazole ring occurred with partial concurrent alkylation at N-1 position (N-2/N-1=2.45), but both alkylated compounds could be readily separated by fractional crystallization. After hydrolysis and full acetylation, the intermediate triacetate at positions 2, 3 and 4 was obtained as an inseparable mixture of the α- and β-anomers in 30:70 ratio by GC analysis. Assignment of the relative stereochemistry of both anomers was based on the coupling constants of their acetalic protons in the ^{1}H NMR spectra and double quantum NMR spectroscopy. Treatment with 2,6-dichloropurine/DBU (1,8-diazabicyclo[5,4,0]undec-7-ene) in the presence of trimethylsilyl triflate afforded exclusively the corresponding β-nucleoside, which was aminated (NH_3/$NaOCH_3$/CH_3OH) selectively at position 6 of the adenosine to afford compound **8** in 32% overall yield from **11**. Reaction of **8** with amino derivatives **12** in *i*-Pr_2NEt (diisopropylethylamine)/DMSO furnished the expected compounds **1**-**7** in variable yields (12-32%, Scheme 1). Racemic amines **12** (**12a**: R=H; **12b**: R=*p*-F; **12c**: R=*p*-Cl; **12d**: R=*p*-Br; **12e**: R=*p*-CF_3; **12f**: R=*p*-OCH_3; **12g**: R=*m*-OCH_3) were obtained in 70-86% yield.[17] For the synthesis of the stereoisomers (*R*)-**6** and (*S*)-**6**, the corresponding amines (*R*)-**12f** and (*S*)-**12f** were obtained by enzymatic kinetic resolution of the racemic compound using *Candida antarctica* lipase B and ethyl methoxyacetate as the acyl donor in 27 and 40% yield and 93 and 97% ee, respectively.

In the course of the optimization reaction conditions of compound **8** with amines **12**, compound **9** was unexpectedly obtained when the reaction was performed on 1-phenylpropan-2-amine (**12a**) in the presence of NaI as catalyst and DMF as solvent at 145ºC for 70 h in 41% yield after HPLC purification (Scheme 1). Formation of this compound can be explained by the nucleophilic substitution of the chlorine atom by N,N-dimethylamine, a known thermal

decomposition product of DMF at high temperatures.[18] Compound **10** was obtained by coupling reaction of 2-chloroadenosine (**13**) with amine **12a** in a mixture of Et_3N/DMSO and NaI as catalyst at 145ºC for 48 h in 36% yield after HPLC purification (Scheme 2).

In general, the new synthetic compounds display a good affinity for the A_{2A}AR in radioligand assays (K_i values in the nM range), moderate for A_3AR and low or almost no affinity for A_1AR and A_{2B}AR (Table 1). This selectivity profile is particularly remarkable for compounds **1**, **4**, **6**, and (*R*)-**6**. As a representative example, the concentration-response curve of compound **1** in the radioligand assays against the A_{2A}AR is shown in Fig. 1A. The affinity of the epimeric compounds tested was not significantly different from that of the corresponding *R* enantiomers (compare compounds **1** with (*R*)-**1**, **4** with (*R*)-**4**, and **6** with (*R*)-**6**)), but the affinity of (*R*)-**6**) was 10-fold higher than that of the (*S*)-**6** enantiomer (Table 1). For the rest of the series, compounds **2**, **3**, **5** and **7** also displayed K_i values in the 10–20 nM range, compounds (*S*)-**6** and **10** showed moderate activity, and compounds **8** and **9** were poor binders for the A_{2A}AR. Interestingly, the two weakest ligands **8** and **9** had a chlorine atom and a dimethylamino group, respectively, at 2-position of the adenosine instead of the phenylethylamino group, suggesting a key role played by this moiety in the accommodation at the A_{2A}AR binding site. In turn, the moderately active compound **10**, bearing the 2-phenylethylamino substituent but lacking the ethyl-substituted tetrazole group at 4'-position of the ribose, displayed a 9-fold decreased affinity as compared to the corresponding derivative **1** containing this moiety (Table 1). This highlights also the importance of the substituted tetrazole for a higher activity.

Introduction of groups of different size and electronegativity (F, Cl, Br, CF_3, OCH_3) in the phenyl ring does not produce in the tested compounds a substantial change in affinity for the A_{2A}AR. It is noteworthy the A_1/A_{2A} selectivity values displayed by compounds **1**, **3**, **4**, **6** and (*R*)-**6** ranging from 53 to 175, and the A_{2B}/A_{2A} selectivity shown by compounds **1** and (*R*)-**1** (74 and 166, respectively) (Table 1). With regard to the binding affinity for A_3AR, compound **8** was the most potent with a good selectivity *vs* A_{2A}AR (A_{2A}/A_3 = 18.5), A_{2B} (A_{2B}/A_3 = 70.6), and A_1AR

(A_1/A_3 = 29). Compounds **1**, **2**, **3**, (*S*)-**6** and **7** were moderate binders for the A_3AR with K_i values lower than 100 nM. As a representative example, the concentration-response curve of compound **1** in the radioligand studies against the A_3AR is shown in Fig. 1B. Interestingly, the absolute configuration of the methyl at 1-position of the phenylethylamino group conveys a substantial change in affinity for this receptor, with the (*S*)-**6** enantiomer being 5-fold more active than the (*R*)-**6** enantiomer, in contrast to the higher affinity of the latter compound for A_{2A}AR, as cited above (Table 1).

Compounds **1**-**6**, (*R*)-**6**, (*S*)-**6**, **9** and **10** were also tested in functional assays as A_{2A}AR agonists and A_3AR antagonists by measuring cAMP formation in transfected CHO cells in comparison to NECA (Table 2). Practically all compounds showed a prominent agonist activity for the A_{2A}AR with derivatives **1**, **2**, **3**, **6**, (*R*)-**6**, and (*S*)-**6** displaying EC_{50} values in 1-10 nM range. As a representative example, the concentration-response curves of compound **1** in functional assays as A_{2A}AR agonist and A_3AR antagonist are shown in Figs. 1C and 1D, respectively. Most of the compounds produced similar amounts of cAMP compared to NECA, suggesting that they all behaved as full A_{2A} agonists (Table 2). Only compounds (*S*)-**6** and **10** showed lower E_{max} than NECA and, therefore, they can be considered as partial agonists. Compounds **1**, **2**, **3**, **5**, (*S*)-**6** and **9** resulted also notable antagonists for A_3AR with K_B in 6-14 nM range. In this assay, the (*S*)-**6** stereoisomer displayed an antagonist activity 2.5-4 fold higher than that of the corresponding (*R*)-**6** stereoisomer and the epimeric mixture **6**, respectively. Modifications in 4' or 5' positions of A_3AR agonists have previously shown to shift their efficacy towards receptor antagonism. These include the presence of 5' groups without hydrogen bond donor groups,[19] analogously to the tetrazole moiety of our ligands. In contrast, receptor agonism was found to be less sensitive to such modifications for other AR subtypes, as exemplified by nucleoside derivatives truncated in the 4' position.[20, 21]

The efficacy of adenosine derivatives on the A_3AR might contrast with that found in the other receptor subtypes and, thus, agonists in the A_1AR were described as A_3 antagonists.[22, 23] The

structural requirements for A_3 receptor activation seem therefore to be divergent to those required for the other receptor subtypes, and some hypothesis based on docking studies of full and partial A_3 agonists have been recently proposed.[24, 25] Our series of A_{2A} agonists with A_3 antagonist activity presents a noteworthy combination with potential therapeutic applications. In this context, it has been reported that (2*R*,3*R*,4*S*,5*R*)-2-(6-amino-2-{[(1*S*)-2-hydroxy-1-(phenylmethyl)ethyl]amino}-9H-purin-9-yl)-5-(2-ethyl-2H-tetrazol-5-yl)tetrahydro-3,4-furandiol (2*Z*)-2-butenedioate (salt), a potent and selective agonist of the human A_{2A} receptor and antagonist of the human A_3 receptor, potently inhibits the infiltration of eosinophils and neutrophils into the lung and, therefore, has been proposed for the treatment of asthma, allergic rhinitis and chronic obstructive pulmonary disorder.[26] However, although the drug improved nasal blockage it had no significant effect on rhinorrhoea, number of sneezes or peak nasal inspiratory flow measurements when compared with placebo.[26] The ligand was also able to inhibit the generation of reactive oxygen species from human eosinophils and the release of preformed granule proteins from neutrophils and eosinophils in human blood.[27]

More recently and in the same context, N6-substituted-4'-thioadenosine derivatives resulted potent ligands as A_{2A}AR agonists and A_3AR antagonists.[21] The most potent compound found, the 2-hexynyl derivative, resulted a potent anti-inflammatory agent on carrageenan-induced paw edema in rats, with the effect being similar to that of indomethacin.[21]

To gain further insight into the structure-affinity relationships we undertook a docking study of our compound series on the A_{2A}AR. The NECA-bound structure of this receptor (PDB code 2YDV)[12] was refined with the molecular dynamics (MD) equilibration protocol implemented in the GPCR-ModSim platform[28] (Supporting Information). This equilibration confirmed the structural role of two crystallographic water molecules in maintaining the agonist bioactive conformation. An equilibrated snapshot of the receptor retaining these water molecules was used for subsequent docking studies with the protein-ligand docking program GOLD[29] (Supporting Information). The full series of compounds reported here were docked, together with the most interesting compounds from the preceding series of agonists,[16] in order to get a

comprehensive SAR of the whole family. The results show a conserved binding mode for the series, consistent with the position of the adenosine scaffold observed in the different A_{2A}AR agonist-bound crystal structures (Fig. 2 and Supplementary Information). This involved a conserved pattern of interactions involving residues Asn253$^{6.55}$ (hydrogen bonds with the exocyclic amine and N7 of adenine), Glu169$^{5.30}$ (hydrogen bond with the exocyclic amine), Phe168$^{5.29}$ (π stacking with the adenine ring), Ser277$^{7.42}$ and His278$^{7.43}$ (hydrogen bonds with 3' and 2' hydroxyls of the ribose, respectively). A number of additional interactions explain the role of the C2 substitutions and the tetrazole group at position 4' of our compound series in their affinity for the A_{2A}AR. The C2 substituent at the adenine moiety points towards the extracellular side, similarly to the (2-carboxyethyl)phenylethylamino group on the C2 position of adenine in the recently crystallised complex of the A_{2A}/A_3AR agonist CGS21680, as experimentally observed in the complex with A_{2A}AR[30] (Fig. 2B). The tetrazole group at position 4' of the ribose establishes a hydrogen bond with His250$^{6.52}$ (Fig. 2A). In addition to this polar interaction, analogous to that observed for the ethylamido group in the NECA-A_{2A}AR crystal structure,[12] our tetrazole substituent makes a π stacking interaction with Trp246$^{6.48}$. These additional interactions can partially account for the high affinity of the current series and the previously reported phenylalaninol series[16] (Fig. S1, Supporting Information). Compound **10**, with a 4'-hydroxymethyl substituent instead of the ethyl-substituted tetrazol, is expected to maintain a polar contact with His250$^{6.52}$ in agreement with the crystal structure of the A_{2A}AR bound to adenosine.[12] Importantly, the two structural water molecules that were retained during the docking explorations revealed to be key for stabilizing polar contacts with these series of agonists, bridging hydrogen bonds between the O2' of the ribose, the N3 atom of the adenine moiety, the NH of the phenylethylamino substituent and the backbone carbonyl of Ala63$^{2.61}$ of the A_{2A}AR (Fig. 2A).

The particular interactions of the agonists here reported are pretty much in line with a recent free energy exploration of agonist binding to the A_{2A}AR.[14] In particular, the lack of potency of

compounds **8** and **9** could be explained by the replacement of the phenylethylamino group by chlorine or the diethylamino moiety, respectively. The flexible phenylethylamino group is important for high affinity, playing a similar role as that in the antagonist ZM241385 or the (2-carboxyethyl)phenylethylamino group of the agonist CGS21680 (Fig 2B). Interestingly, both *R* and *S* isomers at the C1 side chain of the 2 position of the purine ring achieve very similar docking poses (Fig. 2) for compounds **1-7** and **10**. This is in contrast with similar docking analysis of the previously reported phenylalaninol series.[16] In this case, the only molecule tested as epimeric mixture was the *p*-chlorophenyl analogue, which showed several fold reduced affinity than any of the *S* enantiomers reported. It might be assumed then that the *R* enantiomer has somehow lower affinity than the corresponding *S* enantiomer in that compound series. Our docking results are indeed in line with this interpretation of the experimental data and, thus, the hydroxyl group of the hydroxymethyl moiety at 1-position of the phenylethylamino group in the *S* enantiomers of the phenylalaninol series[16] was predicted to hydrogen bond the main chain of Ile66$^{2.64}$ (Fig. S1, Supporting Information).

In summary, a new series of compounds has been prepared as agonists/antagonists of human ARs. In radioligand binding assays, compounds **1**, **4**, **6** and (*R*)-**6** exhibited high affinity (K_i values <10 nM) for A_{2A}AR and prominent A_1/A_{2A} and A_{2B}/A_{2A} selectivity. In functional assays, derivatives **1**, **2**, **3**, **6**, (*R*)-**6**, and (*S*)-**6** showed a significant agonist activity for A_{2A}AR (EC_{50} in 1-10 nM range), and compounds **1**, **2**, **3**, **5**, (*S*)-**6** and **9** resulted also good antagonists for A_3AR (K_B in 6-14 nM range). These results have been supported by molecular docking studies. Our compounds with dual activity as A_{2A}AR agonists and A_3AR antagonists should be added to the plethora of ARs agonists and antagonists with possible therapeutic applications, particularly in asthmatic treatments.

Abbreviations

A_1AR = A_1 adenosine receptor; A_{2A}AR = A_{2A} adenosine receptor; A_{2B}AR = A_{2B} adenosine receptor; A_3AR = A_3 adenosine receptor; cAMP = 3'-5' cyclic adenosine monophosphate; CHO

= Chinese hamster ovary; NECA = 5'-(N-ethylcarboxamido)adenosine; MD = molecular dynamics; GPCR = G-protein coupled receptor; DMSO = dimethyl sulfoxide; DMF = N,N-dimethyl formamide; DPCPX = 1,3-dipropyl-8-cyclopentylxanthine; ZM241385 = (7-amino-2-(2-furyl)-5-[2-(4-hydroxyphenyl)ethyl]amino-[1,2,4]-triazolo[1,5-a][1,3,5]triazine.

Acknowledgements

We thank CSIC for a fellowship to A.R. and Sven och Lilly Lawski Fond for a postdoctoral grant to D.R. We are indebted to Dr. Jordi Bujons (IQAC, CSIC) for advice in the docking studies. This work was supported by the Spanish National Plan for Research and Development (AGL2009-13452-C02-01, AGL2012-39869-C02-01, SAF2011-30104) and the European Regional Development Fund, as well as from the Innopharma project funded by EU Technology Fund, via the Spanish Ministry of Economy and Competitiveness and from Consolidation funds from Xunta de Galicia (GRC2014/011).

Supporting Information

Synthesis and characterization of compounds **1**-**10**. Experimental details for radioligand binding assays and cAMP assays and general guidelines of the molecular modeling studies.

Notes and references

1 G. Cristalli, S. Costanzi, C. Lambertucci, S. Taffi, S. Vittori and R. Volpini, *Il Farmaco*, 2003, **58**, 193.
2 B. B. Fredholm, R. A. Cunha and P. Svenningsson, *Curr. Top. Med. Chem.*, 2003, **3**, 413.
3 K. A. Jacobson and Z. G. Gao, *Nat. Rev. Drug Discov.*, 2006, **5**, 247.
4 J. Linden, *Adv. Pharmacol.*, 2011, **61**, 95.
5 G. L. Stiles, *J. Biol. Chem.*, 1992, **267**, 6451.
6 B. B. Fredholm, A. P. IJzerman, K. A. Jacobson, J. Linden and C. E. Müller, *Pharmacol. Rev.*, 2011, **63**, 1.
7 M. de Lera, Y.-H. Lim and J. Zheng, *J. Med. Chem.*, 2014, **57**, 3623.

8 K. N. Klotz, in *Adenosine Receptors. Therapeutic Aspects for Inflammatory and Immune Diseases*, eds. G. Haskó, B. N. Cronstein and C. Szabó, CRC, Taylor & Francis, Boca Raton, 2007, pp. 1-363.
9 G. Cristalli, B. Cacciari, D. Dal Ben, C. Lambertucci, S. Moro, G. Spalluto and R. Volpini, *ChemMedChem*, 2007, **2**, 260.
10 N. E. Hausler, S. M. Devine, F. N. McRobb, L. Warfe, C. W. Pouton, J. M. Haynes, S. E. Bottle, P. J. White and P. J. Scammells, *J. Med. Chem.*, 2012, **55**, 3521.
11 X. Hou, M. S. Majik, K. Kim, Y. Pyee, V. Alexander, H.-J. Chung, H. W. Lee, G. Chandra, J. H. Lee, S. Park, W. J. Choi, H. O. Kim, K. Phan, Z.-G. Gao, K. A. Jacobson, S. Choi, S. K. Lee and L. S. Jeong, *J. Med. Chem.*, 2012, **55**, 342.
12 G. Lebon, T. Wame, P. C. Edwards, K. Bennett, C. J. Langmead, A. G. W. Leslie and C. G. Tate, *Nature*, 2011, **4743**, 521.
13 F. Xu, H. Wu, V. Katritch, G. W. Han, K. A. Jacobson, Z.-G. Gao, V. Cherezov and R. C. Stevens, *Science*, 2011, **332**, 322.
14 H. Keränen, H. Gutiérrez-de-Terán and J. Åqvist, *PLoS ONE*, 2014, 10.1371.
15 F. Deflorian, T. S. Kumar, K. Pham, Z.-G. Gao, F. Xu, H. Wu, V. Katritch, R. C. Stevens and K. A. Jacobson, *J. Med. Chem.*, 2012, **55**, 538.
16 M. P. Bosch, F. Campos, I. Niubo, G. Rosell, J. L. Diaz, J. Brea, M. I. Loza and A. Guerrero, *J. Med. Chem.*, 2004, **47**, 4041.
17 L. Muñoz, A. M. Rodriguez, G. Rosell, M. P. Bosch and A. Guerrero, *Org. Biomol. Chem.*, 2011, **9**, 8171.
18 W. L. F. Armarego and C. L. L. Chai, eds., *Purification of Laboratory Chemicals*, Elsevier Butterworth-Heinemann, Cornwall, UK, 2003,pp. 609.
19 A. Melman, B. Wang, B. Joshi, Z. Gao, S. Castro, C. Heller, S.-K. Kim, L. Jeong and K. Jacobson, *Bioorg. Med. Chem.*, 2008, **16**, 8546.
20 X. Hou, H. Kim, V. Alexander, K. Kim, S. Choi, S.-G. Park, J. Lee, L. Yoo, Z.-G. Gao, K. Jacobson and L. Jeong, *ACS Med. Chem. Lett.*, 2010, **1**, 516.
21 X. Hou, M. Majik, K. Kim, Y. Pyee, Y. Lee, V. Alexander, H.-J. Chung, H. Lee, G. Chandra, J. Lee, S.-G. Park, W. Choi, H. Kim, K. Phan, Z.-G. Gao, K. Jacobson, S. Choi, S. Lee and L. Jeong, *J. Med. Chem.*, 2012, **55**, 342.
22 Z.-G. Gao and K. A. Jacobson, *Eur. J. Pharmacol.*, 2002, **443**, 39.
23 R. Petrelli, T. I., S. Kachler, L. Luongo, S. Maione, P. Franchetti, M. Grifantini, E. Novellino, A. Lavecchia, K.-N. Klotz and L. Cappellacci, *J. Med. Chem.*, 2015, **58**, 2560.
24 D. Dal Ben, M. Buccioni, C. Lambertucci, S. Sonja Kachler, N. Falgner, G. Marucci, A. Thomas, G. Cristalli, R. Volpini and K.-N. Klotz, *Biochem. Pharmacol.* , 2014, **87**, 321.
25 K. S. Toti, S. M. Moss, S. Paoletta, Z.-G. Gao, K. A. Jacobson and S. Van Calenbergh, *Bioorg. Med. Chem.*, 2014, **22**, 4257.
26 J. Rimmer, H. L. Peake, C. M. C. Santos, M. Lean, P. Bardin, R. Robson, B. Haumann, F. Loehrer and M. L. Handel, *Clin. Exp. Allergy*, 2007, **37**, 8.
27 N. Bevan, P. R. Butchers, R. Cousins, J. Coates, E. V. Edgar, V. Morrison, M. J. Sheehan, J. Reeves and D. J. Wilson, *Eur. J. Pharmacol.*, 2007, **564**, 219.
28 D. Rodríguez, X. Bello and H. Gutiérrez-de-Terán, *Mol. Inf.*, 2012, **31**, 334.
29 M. L. Verdonk, G. Chessari, J. C. Cole, M. J. Hartshorn, C. W. Murray, J. W. M. Nissink, R. D. Taylor and R. Taylor, *J. Med. Chem.* , 2005, **48**, 6504.
30 G. Lebon, P. C. Edwards, A. G. W. Leslie and C. G. Tate, *Mol. Pharmacol.*, 2015, in press.

Captions to Figures

Chart 1. Structures of compounds **1**-**10** as new agonists/antagonists of human adenosine receptors.

Scheme 1. Synthesis of compounds **1**-**9**.

Scheme 2. Preparation of compound **10**.

Fig. 1. Concentration-response curves of compound **1** in A) radioligand binding competition studies at human A_{2A} receptors labelled with [^{3}H]ZM241384; B) radioligand binding competition studies at human A_3 receptors labelled with [^{3}H]NECA; C) cyclic-AMP measurements over basal activity of human A_{2A} receptors; D) cyclic-AMP measurements over 1 μM NECA-activated human A3 receptors in the presence of 10 μM forskolin. Data represent the mean±SD (vertical bars) of duplicate measurements of a representative experiment.

Fig. 2. Predicted binding modes for the most potent A_{2A}AR agonists *(R)*-**6** (**A** and **B**, beige) and *(S)*-**6** (**B**, cyan). The receptor and water MD-equilibrated coordinates of the crystallographic A_{2A}AR-NECA complex (PDB code 2YDV) were used for ligand docking. Direct ligand-receptor hydrogen bonds and water-mediated polar contacts are represented with black and grey dashes, respectively, while π-stacking interactions are shown in magenta. The crystallographic conformation of the agonist CGS21680 bound to the A_{2A}AR (PDB code 4UHR) is shown in dark blue lines in panel **B**.

Table 1 Binding affinity (K_i) of compounds **1**-**10** for human ARs expressed in transfected CHO (A_1AR), HeLa (A_{2A}AR and A_3AR) and HEK-293 (A_{2B}AR) cells in radioligand assays[a]

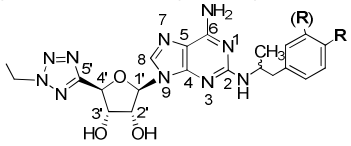

R = H : **1** R = *p*-CF_3 : **5**
R = *p*-F : **2** R = *p*-OCH_3 : **6**
R = *p*-Cl : **3** (*RS*, *R*, *S*)
R = *p*-Br : **4** R = *m*-OCH_3 : **7**

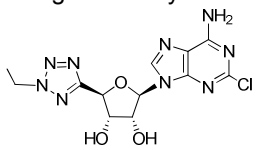

8

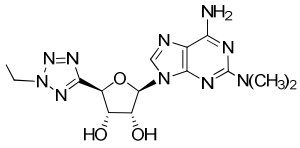

9

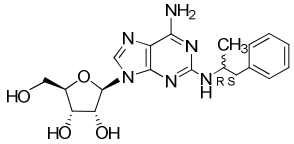

10

Comp.	R	A_1	A_{2A} K_i[c]	A_{2B} K_i[c]/%inh[d]	A_3 K_i[c]	A_1/A_{2A}	A_{2B}/A_{2A}	A_3/A_{2A}
1	H	643±98/__	9.1±0.4	680±225/__	81±13	70.6	74.7	8.9
(*R*)-**1**	H (**R*)	__/56±4	13.2±0.1	2191±499/__	121±41	—	166	9.1
2	F	__/54±3	11.7±0.1	__/45±1	40.6±27	—		3.5
3	Cl	905±140/__	16.1±1.1	__/44±6	55.6±28	56.2	—	3.4
4	Br	1211±127/__	6.9±2.4	__/41±7	228±32	175.5	—	33
(*R*)-**4**	Br (**R*)	__/59±1	10.3±0.1	__/39±1	169±65	—	—	16.4
5	CF_3	__/56±1	16.4±0.1	__/36±1	231±85	—	—	14.1
6	OCH_3	348±205/__	6.5±0.4	__/43±4	122±35	53.5	—	18.7
(*R*)-**6**	OCH_3 (**R*)	340±83/__	5.3±0.1	__/7.6[e]	111±45	64.1	—	20.9
(S)-**6**	OCH_3 (**S*)	881±228/__	56.3±14.6	__/4±3	23±15	15.6	—	0.4
7	*m*-OCH_3	__/45±1	20.9±0.1	__/47±7	75±17	—	—	3.6
8	—	400±99/__	255±96	975±170/__	13.8±1	1.5	3.8	0.05
9	—	1792±457/__	3708±1555	__/14±7	123±31	0.5	—	0.03
10	H	__/27±1	85±0.1	__/22±4	1224±535	—	—	14.4

[a]Binding affinities were determined using [^{3}H]-DPCPX as the radioligand for A_1 and A_{2B}, [^{3}H]-ZM241385 for A_{2A} and [^{3}H]-NECA for A_3. The experimental conditions are cited in the Supplementary Information. Values represent mean ± S.D. from 2-3 experiments.
[b]Unless cited otherwise, **R** refers to the isomer in *para* position. *R* or *S* in italics denotes the absolute configuration of the marked (*) stereogenic center in the general formula of Fig. 1.
[c]K_i values (nM) were calculated by the expression $K_i = IC_{50} / [1+(C/K_D)]$, where IC_{50} is the concentration of compound that displaces the binding of radioligand by 50%, C is the concentration of radioligand and K_D is the apparent dissociation constant of each radioligand.
[d]Percentage of inhibition at 10 μM concentration.
[e]Percentage of inhibition at 1 μM concentration.

Table 2 Agonist potency (EC_{50}) and efficacy (E_{max}) elicited by compounds **1-6**, (*R*)-**6**, (*S*)-**6**, **9** and **10**[a] in comparison to NECA in recombinant human A_{2A}AR and antagonistic potency (K_B) in recombinant human A_{3A}AR expressed in CHO cell lines.

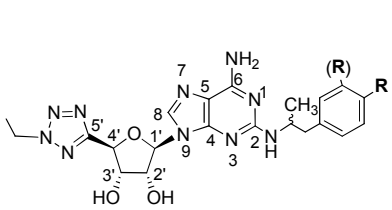

R = H : **1**
R = *p*-F : **2**
R = *p*-Cl : **3**
R = *p*-Br : **4**
R = *p*-CF_3 : **5**
R = *p*-OCH_3 : **6**
(*RS*, *R*, *S*)

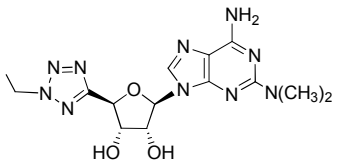

9

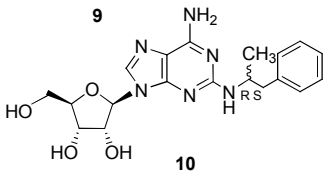

10

Comp.	R	Agonism A_{2A}AR		Antagonism A_3AR
		EC_{50} (nM)[c]	E_{max} (% NECA)[d]	K_B (nM)[e]
1	H	5.5 ± 1.1	100	6.1 ± 2.2
2	F	9.6 ± 3.3	100	6.4 ± 3.1
3	Cl	10.6 ± 4.6	100	10.3 ± 2.8
4	Br	31 ± 4.4	100	27.5 ± 1.7
5	CF_3	19.6 ± 7.2	100	14 ± 1.9
6	OCH_3	4.1 ± 1.5	100	53.6 ± 10.4
(*R*)-**6**	OCH_3 (**R*)	2.2 ± 0.7	100	33.4 ± 6.5
(*S*)-**6**	OCH_3 (**S*)	10.6 ± 3.1	79	14.3 ± 9.2
NECA	—	45 ± 7.7	100	ND[f]
9	—	ND[f]	ND[f]	13.5 ± 4.15
10	H	48 ± 8.1	80	ND[f]

[a]Values represent means ± SEM from two to three experiments.
[b]Unless cited otherwise, R refers to the isomer in *para* position. *R* or *S* in italics denotes the absolute configuration of the marked (*) stereogenic center in the general formula of Fig. 1.
[c]EC_{50} is the concentration of compound that elicited 50% of maximal response.
[d]E_{max} is the percentage of maximal response obtained relative to that observed with NECA.
[e]K_B values were calculated by the expression $K_B=IC_{50}/[(2+([A]/[A_{50}])^n)^{(1/n)}-1]$, where IC_{50} is the concentration of compound that blocks the NECA-mediated inhibition of the forskolin-stimulated increase in cAMP by 50%, [A] is the concentration of NECA employed in the assays, [A_{50}] is the NECA EC_{50} value, and n is the Hill slope of the sigmoidal dose-response curve.
[f]ND = Not determined.

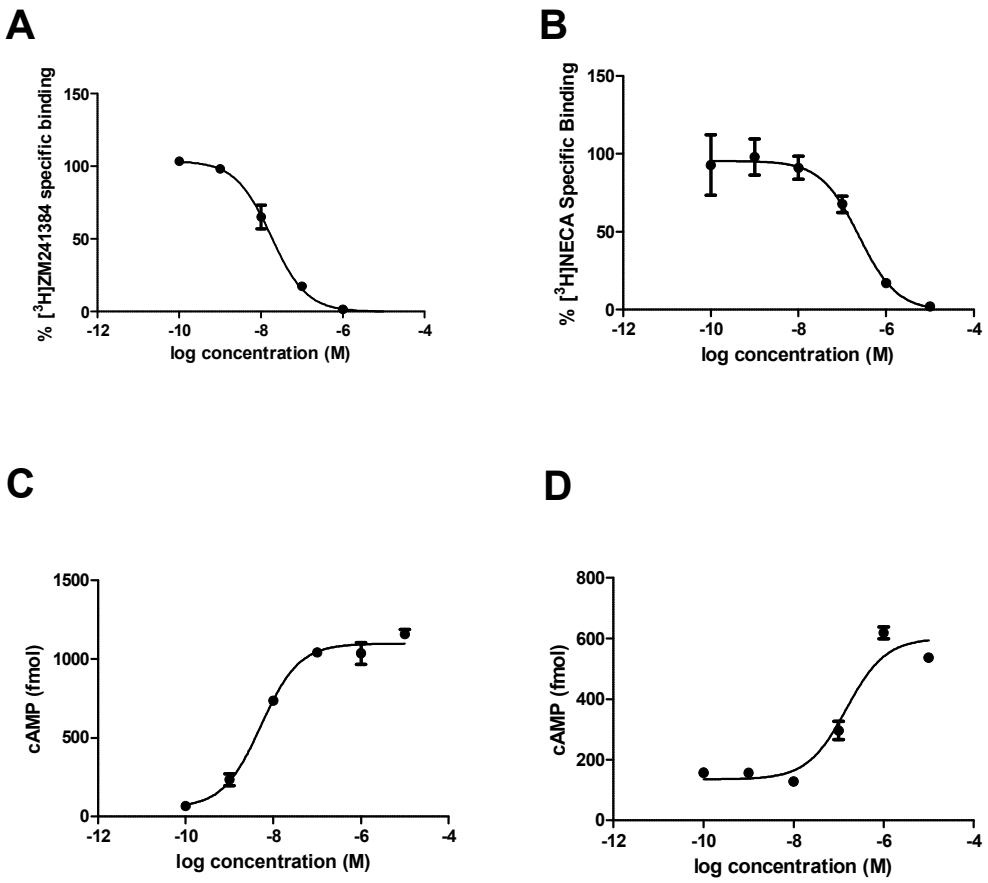

Figure 1

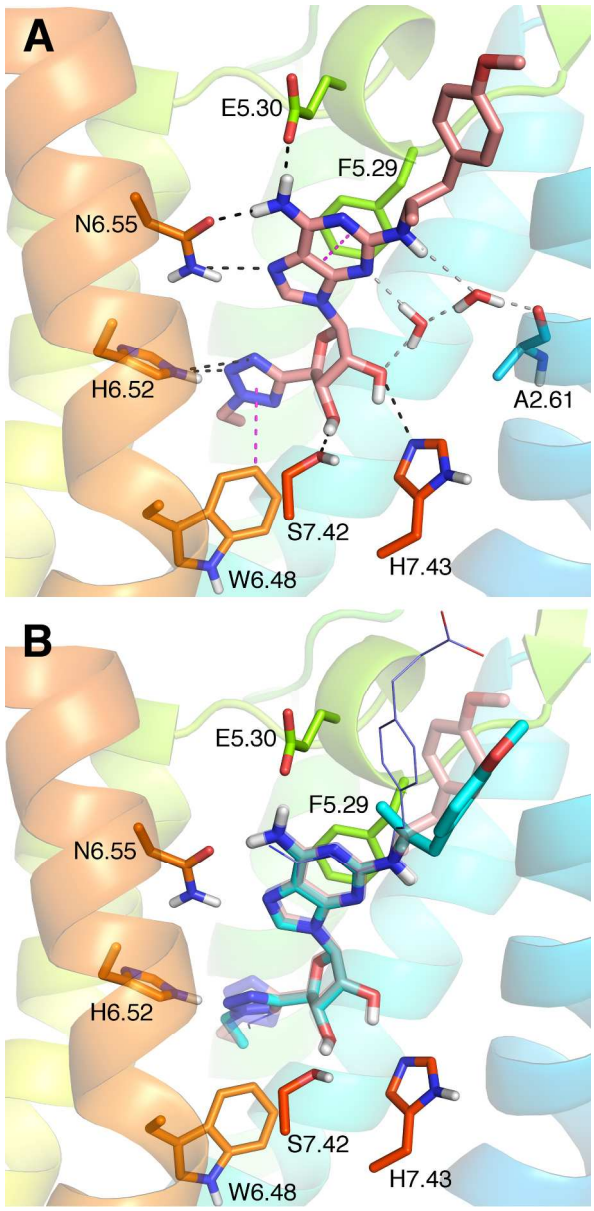

Figure 2
170x349mm (300 x 300 DPI)

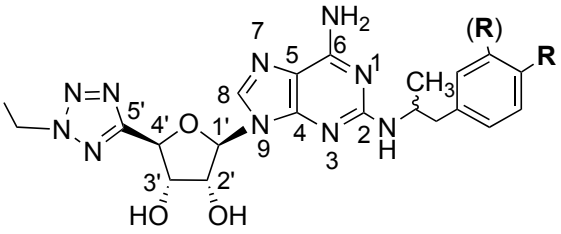

R = H : **1**
R = *p*-F : **2**
R = *p*-Cl : **3**
R = *p*-Br : **4**
R = *p*-CF_3 : **5**
R = *p*-OCH_3 : **6**
(*RS*, *R*, *S*)
R = *m*-OCH_3 : **7**

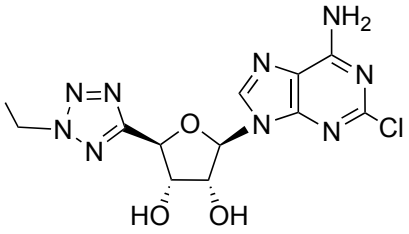

8

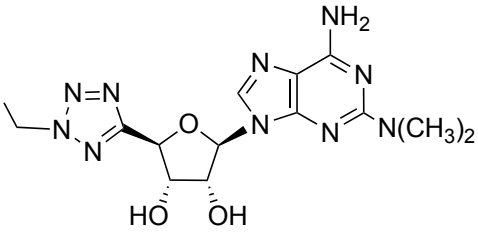

9

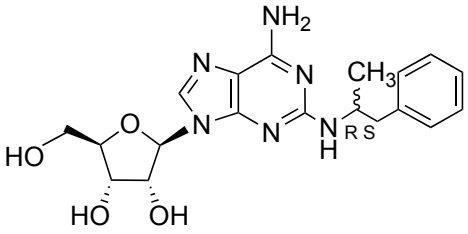

10

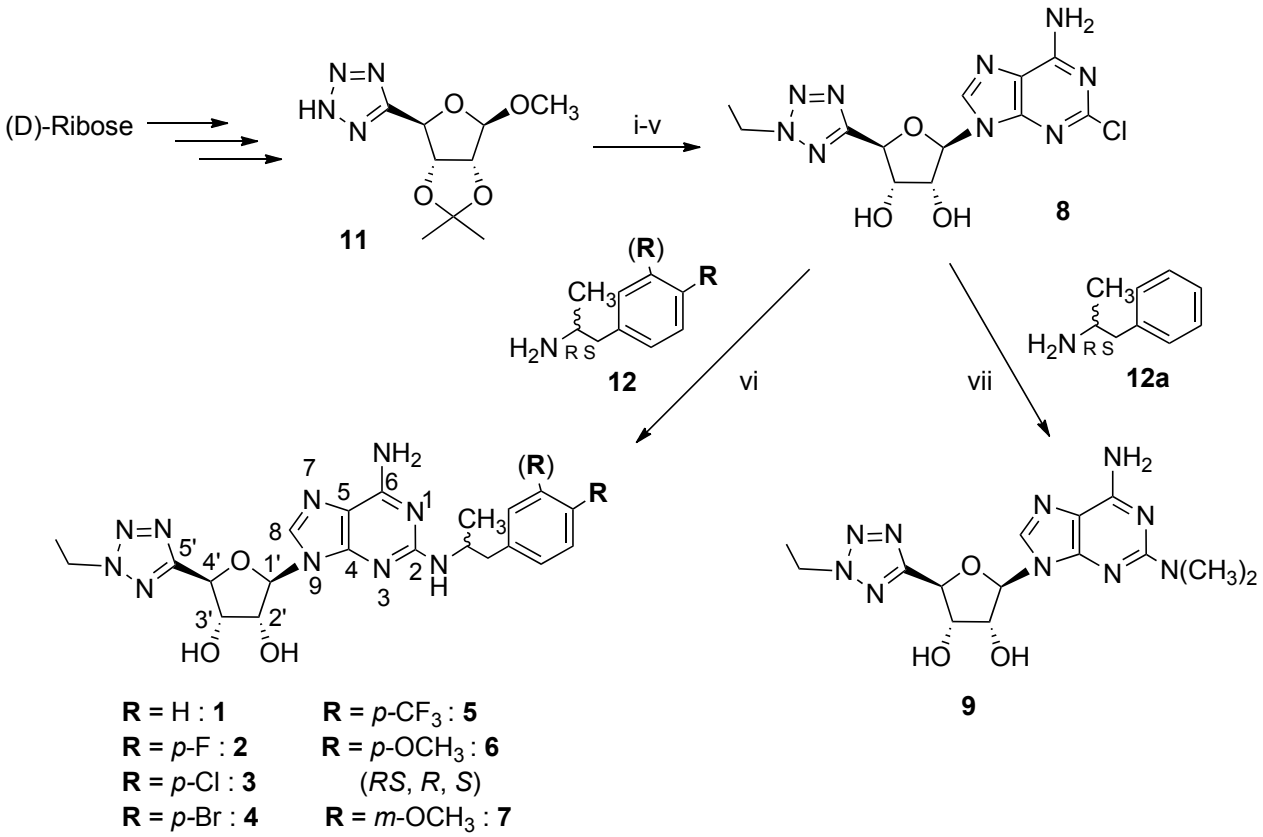

i: EtI, K_2CO_3, acetone, 64%; ii: TFA, H_2O; iii: Ac_2O, Et_3N, DMAP 87%; iv: 2,6-DCP, DBU, TMSOTf, 76%; v: NH_3, THF/$NaOCH_3$, CH_3OH, 77%; vi: *i*-Pr_2NEt, DMSO, 145ºC, 12-32%; vii: *i*-Pr_2NEt, NaI cat., DMF, 145ºC, 70 h, 41%

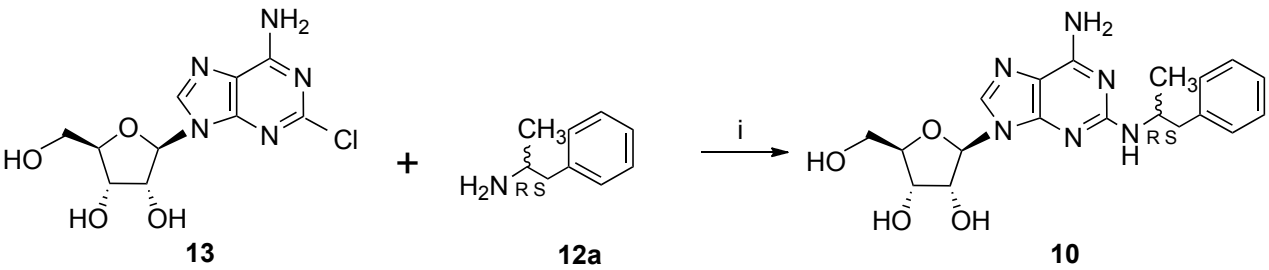

13 **12a** **10**

i: Et_3N, DMSO, NaI cat., 145ºC, 48 h, 36%